PFC/JA-85-21

Plasma Potential Enhancement by RF Heating Near the Ion Cyclotron Frequency

D.K. Smith, K. Brau, P. Goodrich, J. Irby, M.E. Mauel, B.D. McVey, R.S. Post, E. Sevillano, J. Sullivan

June 1985

Plasma Fusion Center
Massachusetts Institute of Technology
Cambridge, MA 02139

Submitted for publication in: Physics of Fluids

Abstract

The observation of enhanced plasma potentials, i.e. potentials greater than the Boltzmann values, in a mirror device is reported. The potential structure is driven by strong radio frequency heating near the ion cyclotron resonance and near the local electron bounce frequency. The potentials and their effect on losses from the central cell of a tandem mirror are discussed.

I. Introduction.

When the trapping and detrapping of electrons in regions of a mirror device are governed by collisional processes the electron distribution tends to be Maxwellian. The potential is therefore described by a Boltzmann relation,

$$q\Phi_B = T_e \ln \frac{n}{n_o},$$

where n_o is the density at the reference point of the potential and n is the local density, q and T_e are the electron charge and temperature, and Φ_B is the potential. Distortion of the local distribution from a Maxwellian results from RF heating and generally yields a stronger Φ vs. n scaling, i.e., potentials which are enhanced over the Boltzman values.[1,2,3] This effect is particularly advantageous when combined with the thermal barrier concept to reduce power flow out of the distorted, or "pumped", region of velocity space.[4,5]

Recent experiments in the TARA Tandem Mirror at MIT have produced convincing evidence of strongly enhanced potentials, $\Phi >> \Phi_B$, driven by RF fields near ω_{ci}, the ion cyclotron frequency, which is also in the range of the local electron bounce frequencies. Recent experiments on the Phaedrus device have shown similar effects.[6]

II. Experiments

The data presented here results from the application of RF power near ω_{ci} by a double half-turn antenna located at the field minimum of the TARA anchor cell. Figure 1 shows the magnetic field along the axis of the device and indicates the various regions of the machine. The anchors are quadrupole mirror cells at the ends of the machine. They have a mirror ratio of two and a minimum magnetic field of 4.7 kG. Fig. 2 shows the anchor magnetic field geometry and location of the antenna with respect to the resonance layer. The resonance position was chosen to correspond to the electron cyclotron heating (ECH) resonance for other experiments and was not optimized for the potential enhancement discussed here.

Operation of the machine for these experiments was as follows. Initially a central cell plasma was formed by ion cyclotron heating (ICH) and ECH. The ion endloss current from this mirror confined plasma flowed out through the anchors which had a density $n_A \simeq 10^{11} cm^{-3}$. At some time, $t = 0$, the ICRF is turned on in the anchor having the immediate effects shown in Fig. 3. Ions from the central cell endloss are trapped at a rate of about 2 amperes in each anchor until $n_A \simeq 3 \times 10^{11} cm^{-3}$. A prompt reduction of endloss ion current measured by Faraday cups occurs within 100 μsec of the ICRF turn-on, much faster than the density build up. The endloss reduction persists in steady state and is larger by several (5 - 10) amperes than the anchor trapping rate implied by the density build up of Fig. 3. The steady state plugging is shown in Fig. 4 along with anchor and

central cell densities. The endloss currents of Fig. 4 are summations of current densities seen by linear arrays of cups extrapolated over the flux tube to get total current within the 5 cm and 12 cm radius central cell flux tubes. The Faraday cups and electrostatic analyzers employ electron repeller grids biased to -600 volts.

The anchor potential Φ_A and endloss energy distribution were obtained from the V-I characteristic of the endloss analyzers as in Fig. 4. The potential, as given by the knee of the curve in Fig. 4, is seen to increase by approximately 200V during anchor ICRF. Central cell swept Langmuir probe measurements show no change in T_e during the plugging and show a rise of only 20-40V in the floating potential Φ_f. Φ_c is generally related to Φ_f as $\Phi_c = \Phi_f + \frac{\alpha}{q} T_e$ where α is a proportionality constant. Since T_e is constant we conclude that the change in Φ_c is also 20-40V, which taken with the data of Fig. 4 indicates a confining potential, $\Phi_A - \Phi_c$, of 150-200V during plugging. Ion endloss analysis made with the ICRF in only one anchor also shows a potential of more than 150V seen from the plugged end and less than 100V seen from the other end consistent with the data of figure 4.

III. Discussion and Conclusions.

Since the anchor density (Fig. 3) is less than the central cell density the Boltzmann relation would predict a value $\Phi_A < \Phi_c$, while the opposite is observed. We emphasize that the observed confining potentials, although subject to the indicated range of uncertainty, are in any case far from the

Boltzmann values. This implies that the RF heating has distorted the anchor electron distribution far from a Maxwellian. Such a strong interaction of the RF fields with the bulk distribution is possible by electron bounce resonance absorption.[2,7]

Bounce resonant absorption by trapped electrons is the Landau damping usually calculated for free streaming distributions considered here in the specific case of electrons bouncing in a local potential well. As in the usual Landau damping, the resonant region of the electron parallel velocity distribution is flattened reducing the number of particles in the distribution which are trapped in a given potential well. Conversely, the result is to raise Φ for a given density. For a combination of parabolic electrostatic and magnetic wells, i.e. of the form

$$B(z) = B_o \left(1 + \frac{z^2}{M^2} (R - 1)\right)$$

$$\Phi(z) = \Phi_o \left(1 - \frac{z^2}{L^2}\right),$$

the electron bounce frequency ω_B is given by

$$\omega_B^2 = \frac{v_\perp^2}{M^2} (R-1) + \frac{2e\Phi_o}{m} \frac{1}{L^2} .$$

Here B and Φ are the magnetic field and potential, M is a magnetic scale length, R is the mirror ratio at the scale length M, $v_\perp$ is the electron

velocity perpendicular to $\underline{B}$ and z is the coordinate parallel to $\underline{B}$. The magnet scale length for R=2 is 50 cm. For $L < M$ and $q\Phi_o > T_e$, the usual case, the second term above is expected to dominate giving only a weak dependence of ω_B on T_e through $v_\perp$. Equating ω_B with the RF drive frequency (7.7MHz) and choosing $v_\perp$ corresponding to a 50eV electron energy implies a scale length L of 18 cm. The distance from the midplane to the ω_{ci} resonance is less than 20 cm for all field lines (Fig. 2) so that 18 cm is a reasonable scale length for RF heating effects.The present data cannot be used to conclusively identify the mechanism of the potential enhancement, however, bounce resonance absorption is plausible. Another possibility is that the RF induces radial transport. Fast radial electron transport in the anchor would have an effect on the potential essentially like that of parallel electron heating. Such transport would have to be ambipolar, however, in order to go undetected by the endloss diagnostics.

Aside from looking at the problem of how the confining potential is formed, we can use the RF induced confining potential as a tool to illuminate other central cell confinement issues. In particular, the present data shows evidence of a strong radial particle loss during the axial plugging. We can define two confinement times

$$\tau_\parallel = \frac{qn_c V}{J_\parallel} \qquad \tau_\perp = \frac{qn_c V}{J_\perp}$$

giving a total particle confinement time

$$\frac{1}{\tau_p} = \frac{1}{\tau_{\parallel}} + \frac{1}{\tau_{\perp}}$$

where V is the central cell volume, $J_{\parallel}$ is the ion endloss current and $J_{\perp}$ accounts for ions not lost from the ends. Typically $\tau_{\parallel}$ is measured at 1-2 msec but increases to more than 10 msec during the plugging. Since there is no large increase in n_c during plugging and there is no evidence for a fueling rate decrease, we must conclude that either $\tau_{\perp} << 1$ msec in general or $\tau_{\perp}$ decreases to ~ 1 msec during the plugging. The latter is much more likely since $\tau_p << 1$ msec would be inconsistent with our estimate of the ionization fueling source which corresponds to $\tau_p \simeq 1.5$ msec. Experimental evidence for an increase in radial losses during plugging includes a neutral pressure rise from 2 to 8 x 10^{-6} torr in the recirculating region between the plug and anchor cells during plugging and an increase in plasma density outside the central cell flux tube in the plug and recirculating regions. The magnitude of these effects is, however, insufficient to account for the reduction in endlosses. The increased radial losses may result from increased low frequency fluctuations which are observed in the plasma edge during plugging or from trapping of ions by ICRF leaking into the recirculating region where poor orbits of trapped particles can lead to radial loss. In normal operation, i.e. plugging potential in the axicell, TARA will have $T_i < q\,\Phi$ in the recirculating region. Under these circumstances the ExB motion maintains the particle drifts near the central

cell flux surfaces so that trapping in the recircularizing region does not lead to radial loss, and additionally the central cell ions do not reach this region. However, in the present experiments, a significant fraction of the central cell ions have access to the region and may be heated by the anchor ICRF to have energy greater than $q\Phi$. In future experiments, the plugging potential will be developed in the axisymmetric plug cell thereby removing the problem of trapping in the recircularizing section.

Figure Captions

Fig. 1 The magnetic field on axis is shown for one half of TARA. The field is symmetric about the midplane (z = 0).

Fig. 2 The anchor mod-B surfaces (dashed) and field lines (solid) are shown with the antenna and resonance locations indicated. Also shown are a diamagnetic loop (D.L.) and cavity employed for electron cyclotron heating.

Fig. 3 Application of the anchor ICRF builds the anchor density by magnetic trapping but endlosses drop on a faster time scale.

Fig. 4 During the anchor ICRF pulse a steady state endloss reduction is observed while the central cell density is constant or rises slightly.

Fig. 5 Collector current - repeller voltage characteristics of electrostatic endloss analyzers indicate the change in temperature of the ions leaving the anchor and the change in anchor potential when the anchor ICRF is applied.

References

1. Cohen, R.H., et. al., Nuclear Fusion 20 (1980) 1421.
2. Smith, D.K., McVey, B.D., Bull. of Am.Phys.Soc. 27 (1982) 915.
3. Cohen, R.H., Phys. Fluids 26 (1983) 2774.
4. Baldwin, D.E., Logan, B.G., Phys. Rev. Lett. 43 (1979) 1318.
5. Grubb, D.P., et al., Phys. Rev. Lett. 53 (1984) 783.
6. Hershkowitz, N., et. al., To be published.
7. Smith, D.K. McVey, B.D., Bull. of Am.Phys. Soc. 28 (1983) 1182.

ACKNOWLEDGEMENT

This work was supported by the U.S. Department of Energy under Grant No. DE-AC02-78ET-51013.

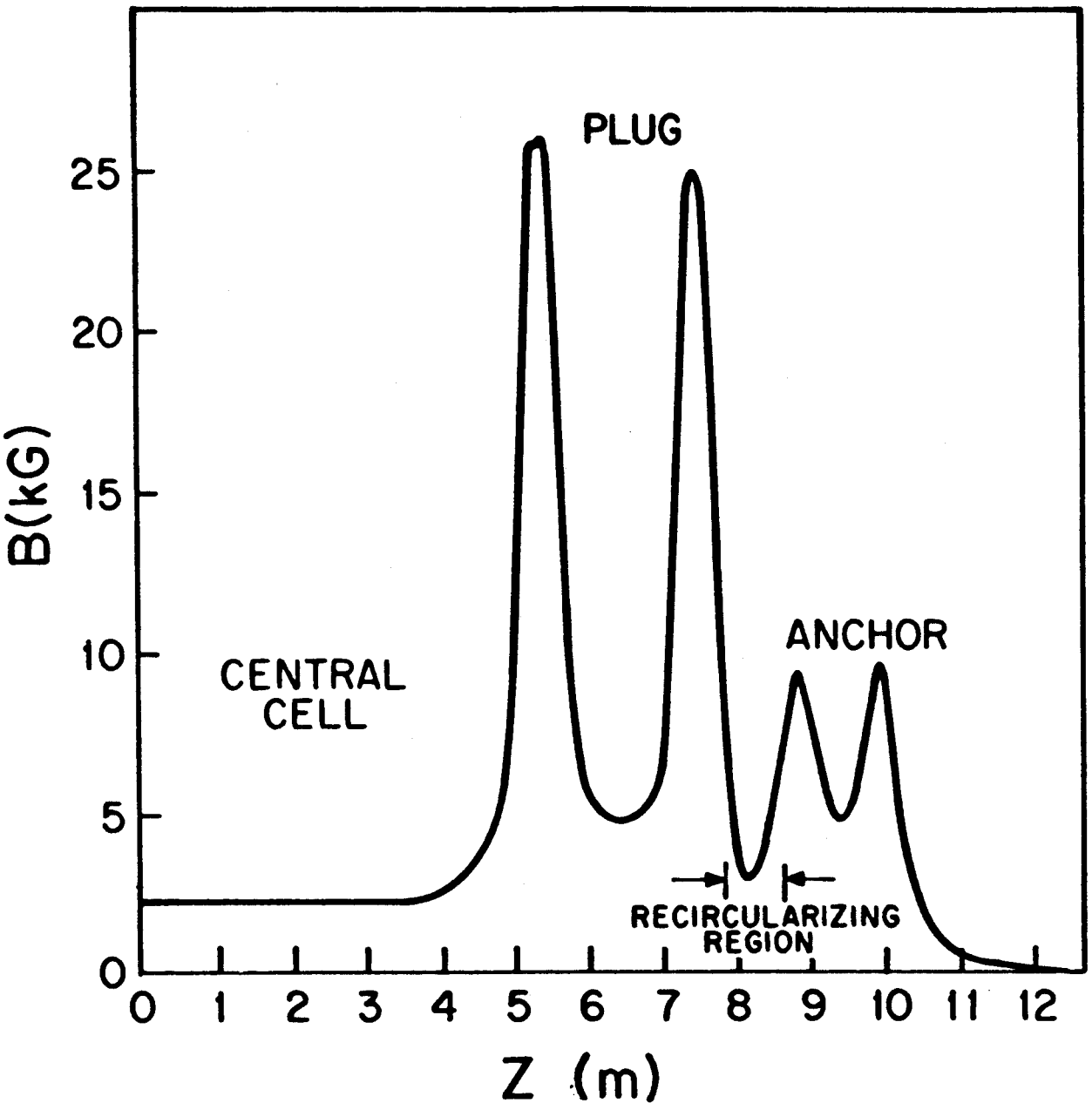
PLUG
ANCHOR
CENTRAL CELL
RECIRCULARIZING REGION
B(kG)
Z (m)
0
5
10
15
20
25
0 1 2 3 4 5 6 7 8 9 10 11 12

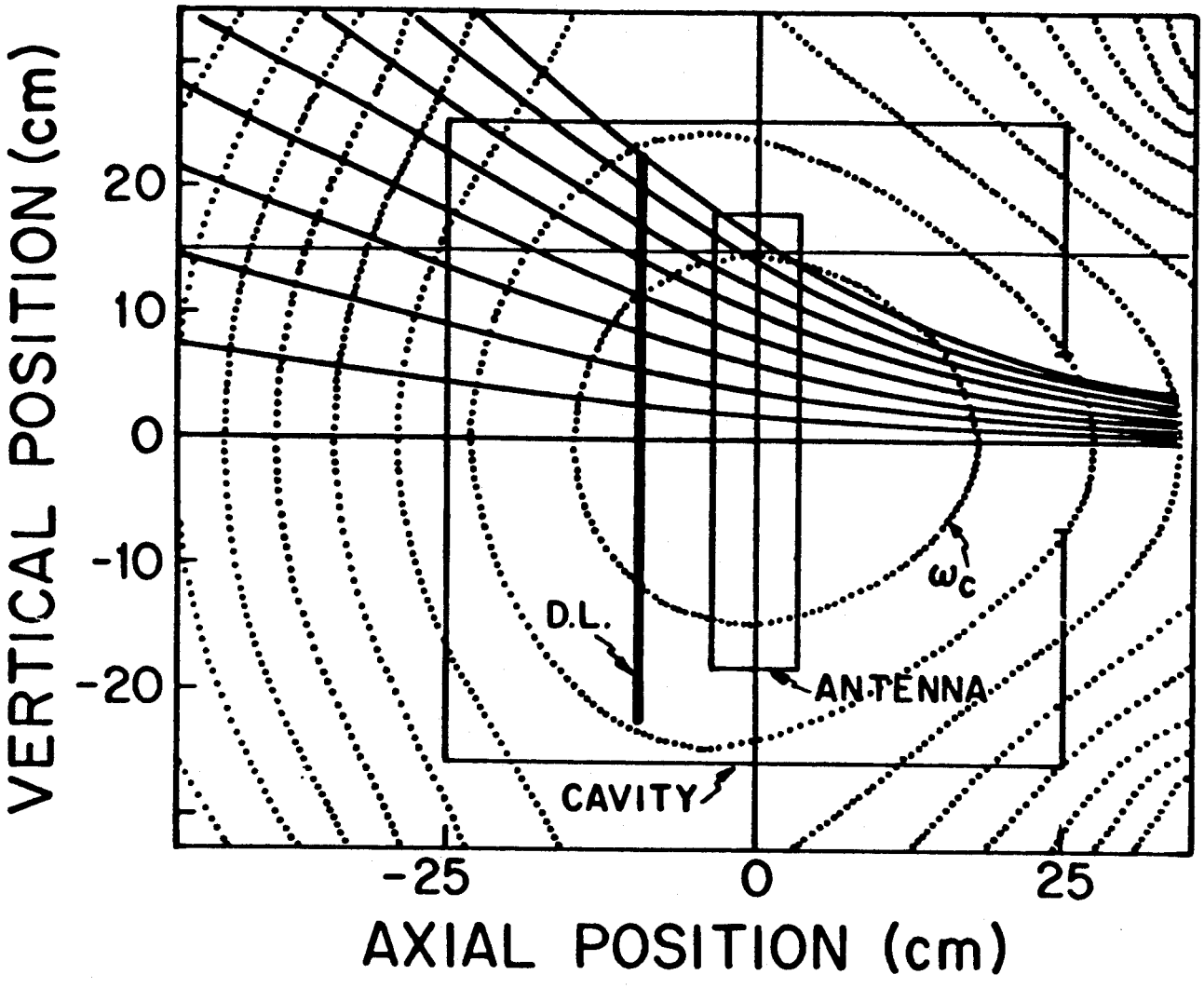

Fig.2 Cross Section of Anchor Cell

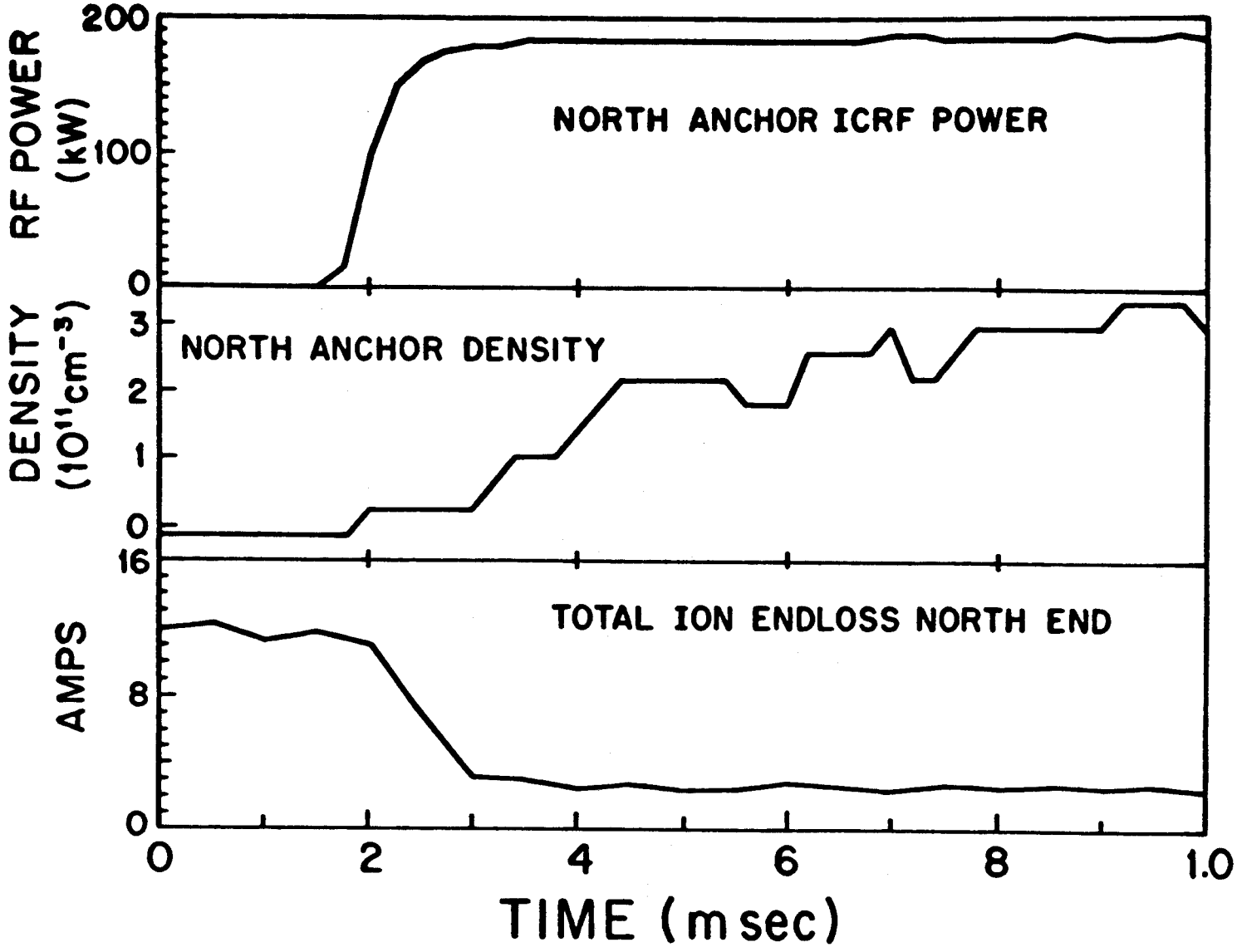

Fig. 3 Fast Endloss Reduction with ICRF

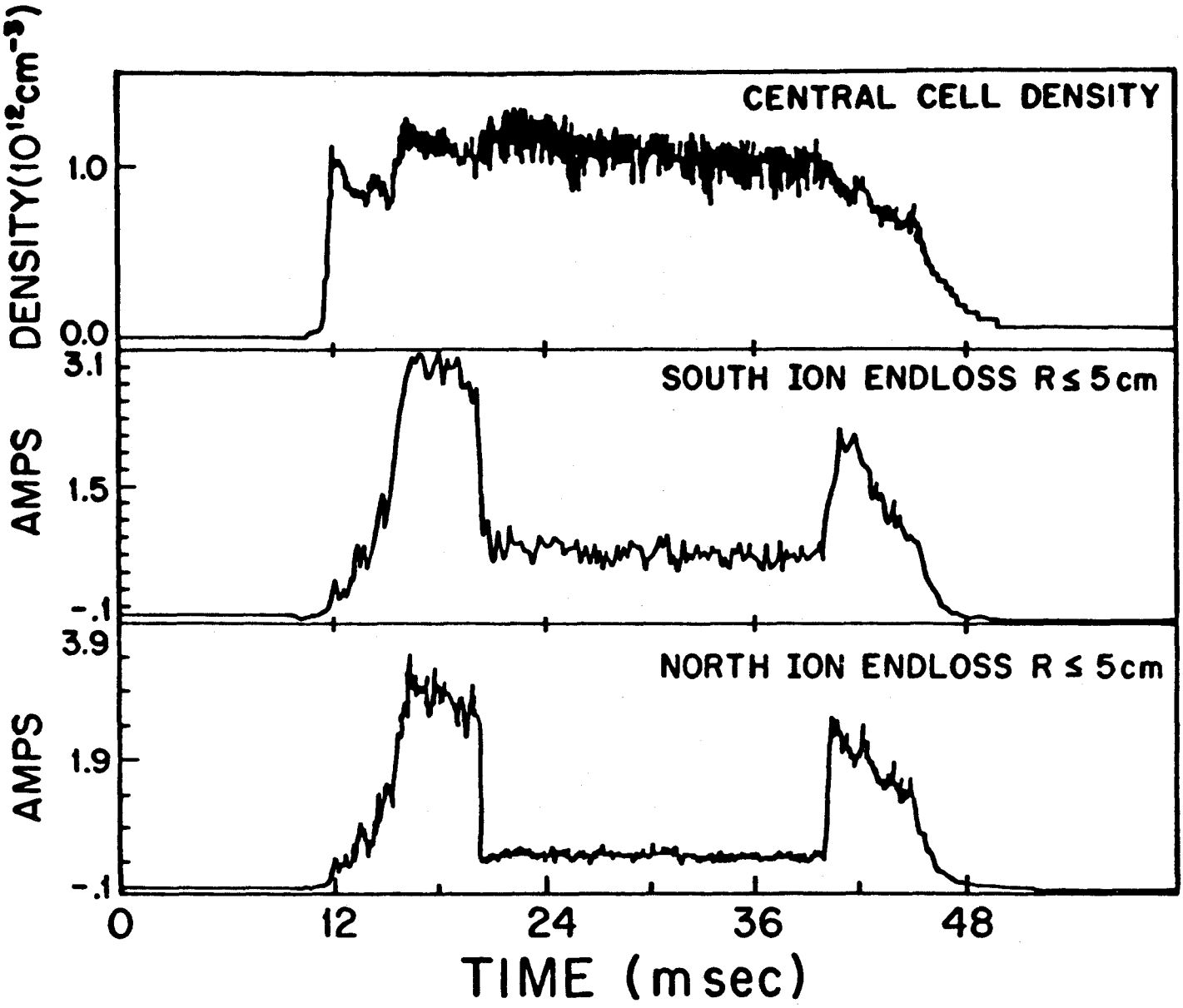

Fig. 4 Endloss Reduction in Steady State

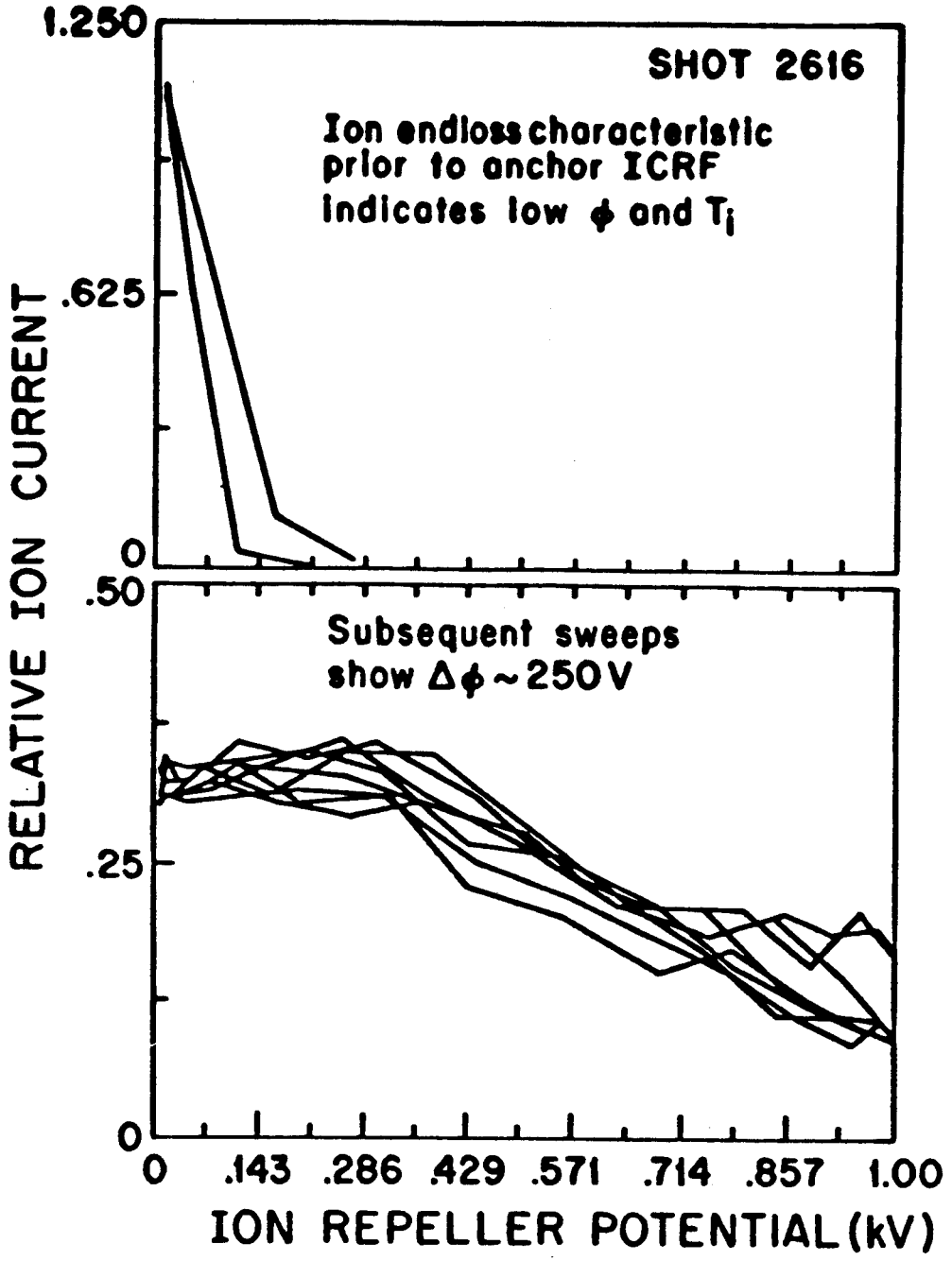
1.250
.625
0
.50
.25
0
SHOT 2616
Ion endloss characteristic
prior to anchor ICRF
indicates low ϕ and T_i
Subsequent sweeps
show Δϕ ~ 250V
RELATIVE ION CURRENT
0
.143
.286
.429
.571
.714
.857
1.00
ION REPELLER POTENTIAL (kV)

Fig. 5